Voltammetric Detection of Cancer Biomarkers Exemplified by Interleukin-10 and Osteopontin with Silica Nanowires

Niranjan S. Ramgir,[†] Aleksandra Zajac,[‡] Praveen K. Sekhar,[†] LaTasha Lee,[‡] Tatyana A. Zhukov,[‡] and Shekhar Bhansali*[,†]

BioMEMS and Microsystems Laboratory, Department of Electrical Engineering, University of South Florida, Tampa, Florida 33613, and H. Lee Moffit Cancer Research Center, University of South Florida, Tampa, Florida 33612

Received: May 2, 2007; In Final Form: July 3, 2007

We report real-time voltammetric detection of potential lung cancer biomarkers, namely, interleukin-10 (IL-10) and osteopontin (OPN), using localized silica nanowires as templates, through an electrochemical alkaline phosphatase (AP) based assay. The high surface to volume ratio associated with nanowires enhances the loading of a specific capture antibody toward a particular cancer antigen. An AP enzyme attached to the cancer antigens (IL-10 and OPN) via detector antibodies hydolyses (dephosphorylates) the *p*-nitrophenyl phosphate substrate to a yellow, water-soluble product, *p*-nitrophenol (pNP). This was detected in a small test volume of 3 μL, using a microelectrode cell fabricated in Au. The electro-oxidation of pNP occurs between 0.85 and 0.9 V with anodic peak current showing linear dependence with the capture antibody and antigen concentrations, respectively. The detection of IL-10 down to 1 fg/mL in ideal pure solution and 1 pg/mL in clinically relevant samples was achieved reproducibly. Moreover, both the concentration of the capture antibody and the cancer antigen were found to have a strong influence on the anodic peak current, as demonstrated considering specific example of OPN.

1. Introduction

With the advent of micro/nano electro mechanical systems (MEMS/NEMS) there has been an upsurge in the development of miniaturized devices using the novel class of materials commonly referred to as nanomaterials.[1−3] The high surface to volume ratio, coupled with the larger density of defect states on the nanomaterials, makes them highly sensitive to minor surface perturbations (i.e., binding chemistry). This could result in a sensor with a high degree of selectivity and sensitivity and a unique chemical signature. Among the one-dimensional nanoentities, silica nanowires (SiO_2-NW) have been widely studied because of their unique anisotropy in physical, optical, electronic properties with excellent photoluminescence and biocompatability.[4−6] Moreover, the nanowires' surface can be easily and effectively modified with the well-known chemistry of Si, thereby allowing the creation of a label-free platform for more sensitive detection of marker level. Its surface has been immobilized with various biomarkers; for example, the addition of fluorescent dyes and oligonucleotides to the nanowires has been achieved by means of chemical grafting at their 3′-terminus (amino linker).[7−8] Consequently, it has been looked upon as a potential candidate in biomarker-based microanalysis systems, hence lending themselves as contrast enhancement agents.[9−10]

We have demonstrated earlier the site specific growth of SiO_2 nanowires using a metal (Pd, Pt, and Au) seeded vapor−liquid−solid (VLS) mechanism.[11−12] Moreover, the ability to control the site and morphology, coupled with simple surface modification chemistry of nanowires, has been employed for developing sensors with enhanced performance.[13−14] Accordingly, in the present work, we demonstrate the applicability of the SiO_2-NW as an effective template in the enzyme immunoassay for voltammetric detection of two potential lung cancer biomarkers—the immunoregulatory cytokine, interleukin-10 (IL-10), and a cell signaling glycoprotein, osteopontin (OPN). Cytokines are proteins with the ability to stimulate or inhibit cell growth, regulate cell differentiation, induce cell chemotaxis, and modulate the expression of other cytokines. Generally, in tumors there is a shift in the balance of expression of cytokines, resulting in enhanced cell proliferation, angiogenesis, and metastasis. They can also block immune-cell-mediated mechanisms for identifying and destroying tumor cells and may be indicative of a poor prognosis. Proinflammatory cytokines such as TNF-α and a number of different interleukins have been identified as orchestrating a preneoplastic process in a number of cancers.[15] For certain types of cytokines, such as IL-1-β, IL-6, IL-8, TNF-α levels were reported to increase in sera of cancer patients compared with healthy controls, while for other types, such as IL-10, decreasing levels were found with cancer.[16] The subtle differences require supersensitive and specific methods for their detection. IL-10 is a homodimeric protein biomarker often

SCHEME 1: Sandwich Electrochemical Immunoassay Protocol

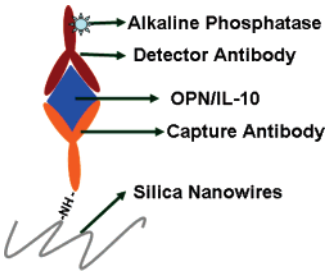

* Corresponding author. E-mail: bhansali@eng.usf.edu.
[†] BioMEMS and Microsystems Laboratory.
[‡] H. Lee Moffit Cancer Research Center.

10.1021/jp073371b CCC: $37.00
Published on Web 08/24/2007

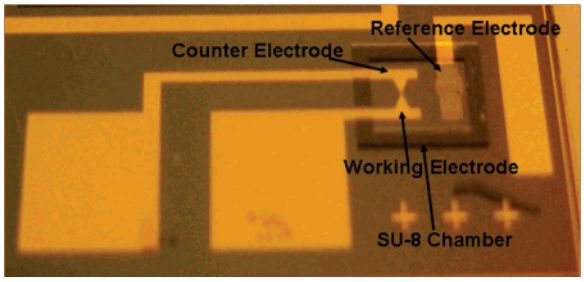

Figure 1. Optical image of the electrochemical cell used for the detection.

associated with various carcinomas, chronic inflammatory bowel ailment, and many more diseases, and hence its detection is very crucial for diagnostic and therapeutic purposes.[17−19]

OPN is a phosphorylated, integrin-binding, transformation-associated glycoprotein with diverse functions, including cancer development, progression, and metastasis. Its expression is induced by a variety of stimuli, including TNF-α and Ras proto-oncogene.[20] Little is known about the significance of OPN expression in human cancers. Findings suggest that CD44 acts as a cell surface receptor for OPN and hyaluronate. It was shown that expression of isoform CD44S is altered in non-small-cell lung cancer (NSCLC), suggesting that CD44S down-regulation may confer a protective advantage of allowing escape from tumoricidal effector cells, including activated macrophages and OPN produced by them. Differential OPN expression and its regulation in each histologic type of lung cancer are not well established. Available data suggest that OPN is especially expressed among squamous cell carcinoma of the lung with less frequency in other histologic types of NSCLC. Ras-p21 was shown coexpressed with OPN, which may suggest that OPN expression is tightly regulated by Ras oncogene, and its concomitant induction with Ras activation may play a crucial role in the development of squamous cell carcinoma of the lung.

The specific bonding between the antibody and antigen, coupled with the enzymatic reaction between the alkaline phosphatase (AP) enzyme attached to the cancer antigen and the *p*-nitrophenyl phosphate (pNPP) substrate, helps to improve both the sensitivity and selectivity of the assay. AP hydolyses (dephosphorylates) the substrate pNPP to a yellow, water-soluble product, *p*-nitrophenol (pNP), that has a characteristic absorbance at 405 nm.[21] pNP can also be detected by electrochemical reduction of its aromatic nitro group or by oxidation of its aromatic hydroxyl group. The pNPP/pNP couple is the most widely exploited, considering the fact that the chromogen pNP can be easily quantified with absorbance enzyme linked immunosorbent assay (ELISA) plate readers. In the present work, we report the electrooxidation of pNP using a Au microelectrode cell as a tool to determine the concentration of cancer antigens in the test as well as clinically relevant samples.

2. Experimental Details

2.1. Materials. Gold was purchased from Sigma Aldrich and SU-8 resist was from Microchem Corp. (Newton, MA). The capture antibody rat antihuman IL-10 (IgG1; JES3-9D7, cat. MCA1531), the detector antibody biotinylated rat antihuman IL-10 (IgG2a; JES-12G8, cat. MCA2250), and the recombinant human IL-10 antigens (cat. PHP047A) were purchased from AbD Serotec, UK. Human osteopontin antigen peptide (cat. 908−049), the capture antibody anti-human osteopontin mouse IgG monoclonal (cat. 905−078) and the detector antibody anti-human osteopontin, rabbit IgG affinity (cat. 915−034) were purchased from Assay Designs Inc. Protein array blocking agent was purchased from Whatman. The streptavidin-coated quantum dot (QD-655) (6−10 nm) fluorescent tag was purchased from Molecular Probes, Inc. The streptavidin-coated alkaline phosphatase enzyme and *p*-nitrophenyl phosphate liquid substrate system (combines *p*-nitrophenyl phosphate, buffer, and the required magnesium cations in a convenient ready to use, single solution reagent), Tris buffer (pH = 9.2), phosphate buffer solution (PBS) (pH = 7.2), 3-aminopropyltrimethoxysilane (APTMS), and ethanol were purchased from Sigma Aldrich. The preclinical lung serums were collected from participants in the lung cancer screening helical clinical trial (CT) at the Moffitt Cancer Center.

2.2. Site-Specific Nanowire Synthesis. Silica nanowires were synthesized on Si substrate using the vapor−liquid−solid (VLS) mechanism.[11−12] Prime-grade 2 in. n-type silicon wafers were used as a substrate for subsequent Pd deposition. The wafers were subjected to a standard RCA cleaning process prior to use. Palladium was reactively sputtered on silicon at a power of 50 W with a constant presputtering of about 4 min. A base pressure of 1.33×10^{-4} Pa and a working pressure of about 2.66×10^{-2} Pa were employed for deposition. The desired selectivity was achieved through a rectangular shadow mask, covering half the area of the wafer. Subsequently, the Pd-deposited Si wafer was diced into 12×12 mm^2, kept on a blank Si wafer (2.54 cm^2), and heated in an open-ended quartz tube furnace (4 in. MB 71 Mini Brute Tube furnace, Thermo Products, CA) with Ar as a carrier gas (flow rate 30 sccm). Finally, the growth of nanowires was accomplished using a three-step process; initially the furnace was ramped to 1100 °C in the presence of Ar atmosphere and then the sample was introduced and heated for 1 h, followed by natural cooling to room temperature.

2.3. Surface Modification of Nanowires. The substrates with patterned nanowires were transferred into a glass vial containing 2% solution of APTMS in ethanol. APTMS precipitates onto silica substrates generating a high concentration of reactive primary amine groups that are evenly distributed across the surface.[8] For this, the wires were soaked in the aliquot for 1 h and then rinsed with ample ethanol for 5 min.

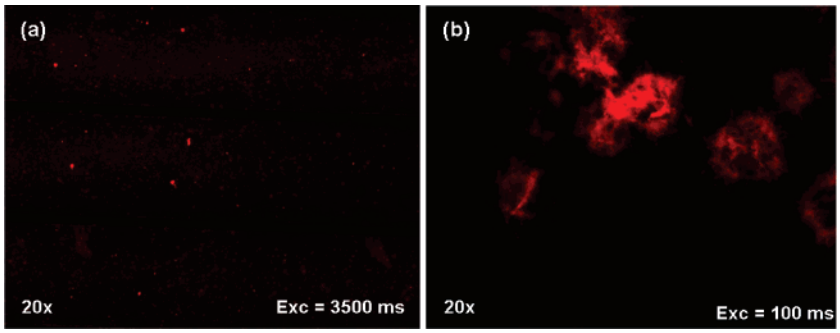

Figure 2. Fluorescent image recorded for (a) Au-patterned planer SiO_2 and (b) SiO_2-NW after performing the whole assay procedure.

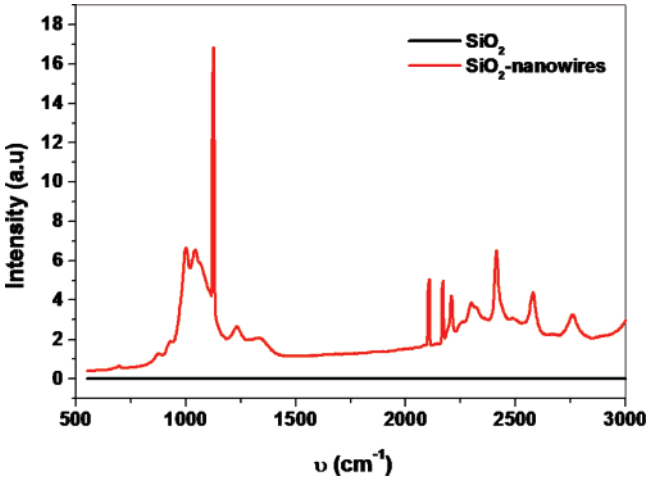

Figure 3. Surface-enhanced micro-Raman spectra recorded for planer SiO_2 and SiO_2-NW after performing the assay till IL-10 antigen attachment.

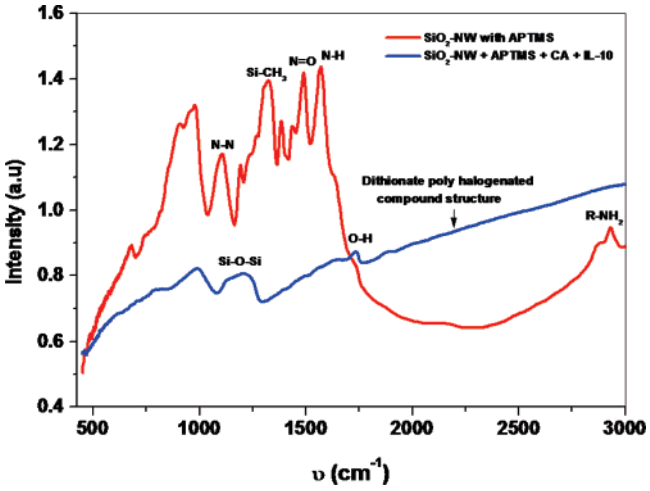

Figure 4. FTIR spectra recorded for the SiO_2-NW after modification with APTMS and after attaching IL-10 antigen.

Further, a standard "sandwich" immunodetection methodology optimized in previous studies on development of protein microarrays with quantum dot (QD) nanoprobes is used.[22] The immunoassays were performed at pH 7 using phosphate buffer solution. The protocol as illustrated in Scheme 1 involves the following steps: (a) deposition of capture antibody for IL-10 antigens, followed by overnight incubation at 4 °C; (b) application of a protein array blocking solution in order to control the nonspecific binding, followed by 2 h incubation at room temperature in humid conditions; (c) immobilization of IL-10 antigens, by incubation for 2 h at room temperature; (d) attachment of a biotinylated detector antibody by incubation for 2 h at room temperature; (e) attachment of a streptavidin-coated alkaline phosphatase enzyme by incubation for 30 min at room temperature; (f) finally, 30 μL of pNPP solution was added to the chamber and the enzymatic reaction was allowed to proceed for 20 min in the dark at room temperature under humid conditions.

The reaction was stopped by adding 50 μL of PBS stopping solution. The stopping solution results in the change of pH and the addition of a high concentration of phosphates (an alkaline phosphatase inhibitor), enough to stop the reaction. The product of the reaction, pNP, was then collected in a vial and used for electrochemistry. After every step from a to c the chamber was washed thoroughly three times, each at a 5 min interval with

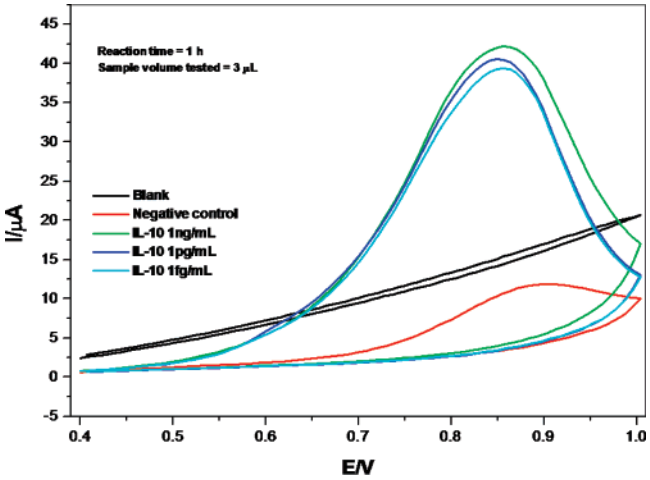

Figure 5. Voltammograms recorded for the reaction product pNP (3 μL) collected with different concentrations of IL-10 antigen in Tris buffer solution with an incubation time of 1 h at scan rate of 50 mV/s vs Ag as the reference electrode.

PBS to remove any nonspecific binding. Similarly, after the steps d and e, the chamber was washed thoroughly with Tris buffer. Both the concentrations of capture antibodies (1 μg/mL to 1 pg/mL), which corresponds to the concentration of 10 mM to 10 μM, and the IL-10/OPN antigens (1 ng/mL to 1 ag/mL) were varied to estimate the detection limits of the proposed scheme and to find the optimal subset of parameters for the detection.

2.4. Electrochemical Cell Fabrication. The microfluidic device as shown in Figure 1 was fabricated in oxidized (100) silicon substrate. The electrodes were fabricated on a thermally oxidized silicon wafer in Au. This was accomplished by photolithography, subsequent e-beam evaporation and lift-off of Cr/Au layers. Cr (300 Å) was used as the adhesion layer for Au (1500 Å). One of the Au electrodes was plated with Ag for use as a reference electrode for the small volume samples. Microelectrodes are uniquely suited for the detection of the electrochemically reversible systems, for at moderate scan rates the nonplaner diffusion between the electrodes gives rise to steady-state currents. Such amplification of the limiting current by redox cycling has been effectively employed for improving the lower detection limit.[23] A 60 μm tall microfluidic chamber of SU-8 (3 × 2 mm) (Microchem Corp., Newton, MA) was finally fabricated to hold the reagents. The SU-8 chamber was then hard-baked at 180 °C for 3 min to prevent any outgassing or contamination.

2.5. Electrochemical Setup. All cyclic voltammetry was performed in a homemade cell with a total volume of 3 μL using an Autolab PGSTAT30 from Eco chemic N.V, at room temperature (Figure 1). A standard three-electrode configuration was used, in which the Au microelectrodes worked as both the working and the counter electrode, while the reference electrode was fabricated by depositing Ag on one of the Au electrodes. The use of a Ag-plated electrode in the miniaturized electrochemical cell is not a problem for the quantitative determination, as also demonstrated by Heineman et al.[24] pNPP was used as a substrate for electrochemical detection with AP enzyme, a useful enzyme for the heterogeneous electrochemical enzyme immunoassays.[25] One AP unit hydrolyzes 1 μmol of pNPP per min at pH 9.8 and 37 °C. The incubation time was also varied to establish the optimum working conditions.

2.6. Optical Studies. Fluorescent microscopy (Nikon Eclipse E800) with custom image analysis was used to detect the molecular signature binding. For QD655 we have used 415 nm

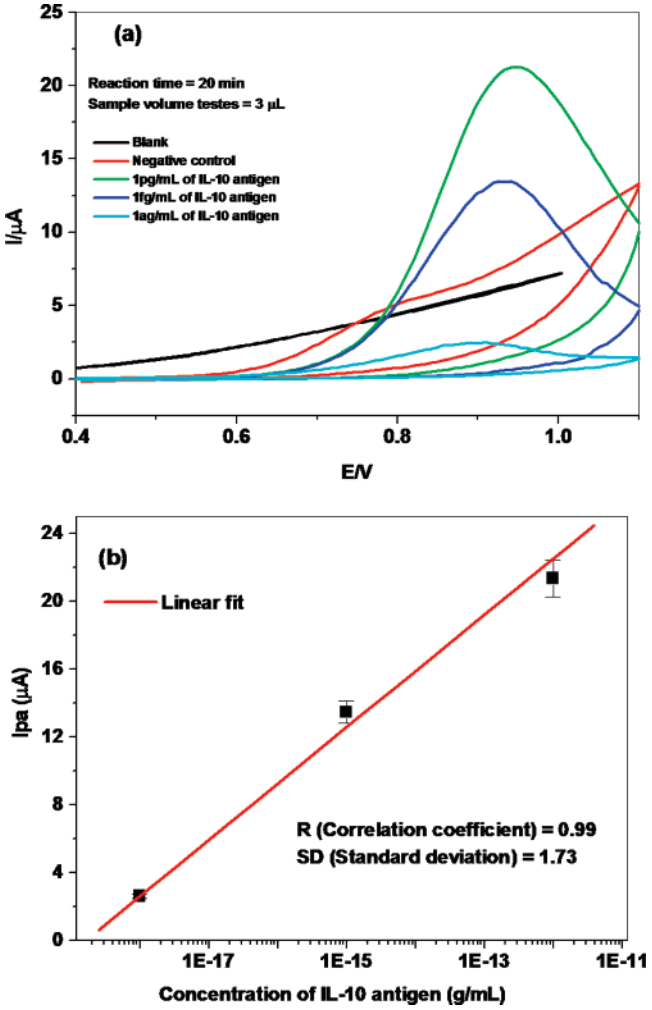

Figure 6. (a) CV recorded with incubation time of 20 min and (b) the linear dependence of anodic peak current on the concentration of IL-10 antigen used.

excitation and 655 nm emission wavelengths. Additionally, micro-Raman (ReniShaw) spectroscopy was used to sequentially capture the microcosm of functional groups, signature traces of CA, and footprints of IL-10 using Ar (514.5 nm) laser excitation at 24.6 mW averaged over two cycles of 10 s exposure. After every routine of Raman, the samples were inspected under the Perkin-Elmer PE1600 FTIR (Fourier transform infrared) spectrometer, in the range of 400−4000 cm^{-1} at a resolution of 1 cm^{-1} for the complimentary infrared absorption using a sealed and desiccated optical module.

3. Results and Discussion

Scheme 1 shows the assay protocol used in the present study. Silica nanowires were first surface-functionalized with APTMS to generate free $-NH_2$ groups over its surface, to which capture antibody specific toward a particular cancer antigen was immobilized. These capture antibodies in essence captured the antigens present in the test samples, which were then detected by immobilizing the detector antibody attached to an electrochemical probe, i.e., AP enzyme. AP hydrolyzes the substrate pNPP to pNP which is then collected and used for electrochemical measurements.

The binding chemistry of the IL-10 antigen to the detector antibody was confirmed using QD-655 as a fluorescent tag. As shown in Figure 2, florescence was observed with nanowires at an excitation of 100 ms; however, for planer SiO_2 an excitation of 3500 ms was required to identify the reaction. No significant binding could be optically observed in the SiO_2 sample as compared to that of SiO_2-NW at the same excitation level. This implies that the total process is highly specific and the presence of nanowires helps in improving the sensitivity toward IL-10 antigens.

Raman and FTIR investigations were also carried out to further establish the chemical binding protocol. Visible Raman spectrum of silica nanowires after performing the whole assay displayed the characteristic D2 defect mode at around 697 cm^{-1}, congruent with the Si−O−Si stretch and a shifted trisiloxane D1 mode around 1120 cm^{-1} (Figure 3).[26] A peak pattern from 864 to 1230 cm^{-1} could be attributed to the intrinsic surface phonon activity in accordance with the earlier reports.[27] Moreover, the signature group frequencies from 2000 to 2500 cm^{-1} arising from the nanocomposite can be attributed to interfacial behavior, coupled with charge transfer associated with the antibodies. In particular, the Stokes lines emerging from 2150 cm^{-1} (N−H stretch) seems to be a result of complete participation of nanowires with the bidentate APTMS molecules. Additionally, appearance of a distinct sharp peak around 2105 cm^{-1} suggests IL-10 binding to nanowires forming a complex moiety.

In order to further confirm the effective binding in the test protocol the FTIR spectra were recorded for the nanowires with APTMS and IL-10 antigen, respectively (Figure 4). The broad peak in the range of 925−1105 cm^{-1} could be due to the asymmetric stretching of Si−O−Si or Si−O−C (1014−1090 cm^{-1}) bond. An absorption band for Si−O−Si is an indication of existence of polysiloxanes deposited onto the nanowires surface. A sharp CH_2 rocking mode around 940 cm^{-1} and the propyl ammonium group, more pronounced with N−N, N−H,

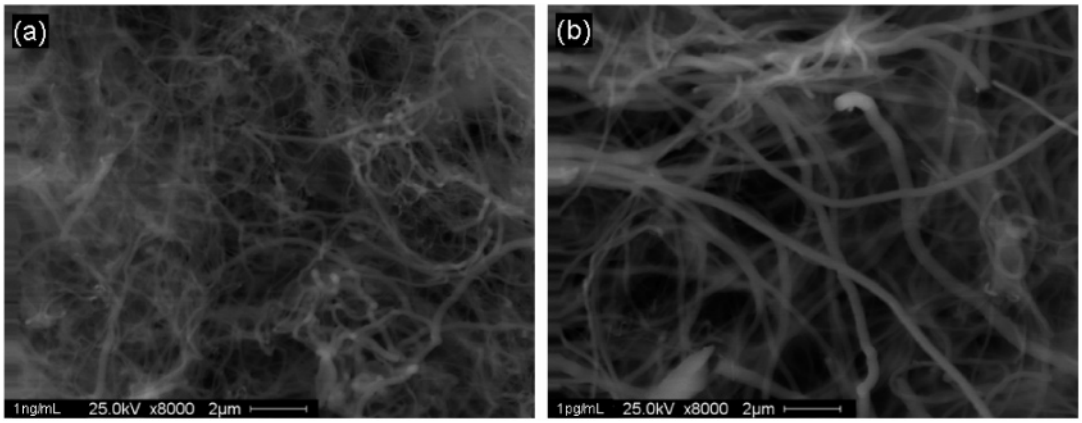

Figure 7. SEM images of the samples used for the testing of IL-10 concentrations (a) 1 ng/mL and (b) 1 pg/mL, respectively.

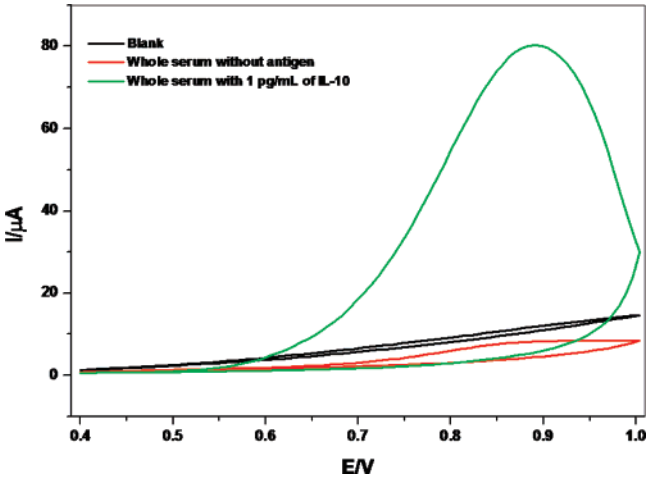

Figure 8. CV plot recorded for the whole serum samples without and with 1 pg/mL concentration of IL-10 at a scan rate of 50 mV/s.

and N═O functionalities, were observed for nanowires with APTMS. A decrease in absorbance characterized by the formation of a polycarbon compound structure formed as a result of complex IL-10 antigen−antibody binding was also visible. A distinguished peak around 1200 cm^{-1} could be attributed to the Si−O−C bond. This corresponds to the condensation reaction between the antigen and the silane.[27] These results confirm the effective chemical binding involved in the testing protocol.

A standard immunosorbent assay protocol that exhibited a high specificity toward IL-10 having no cross reactivity with other proteins was used.[21] The high specificity has been exploited in the present work for realizing the small volume voltammetric detection of IL-10. The enzymatic reaction product pNP is electroactive and underwent an irreversible oxidation between 0.8 and 0.97 V (vs Ag pseudoreference electrode) in 0.1 M Tris buffer when a potential scan from 0.5 to 1.1 V at a scan rate of 50 mV/s is applied.[22] The conversion reaction of pNPP to pNP under the influence of AP enzyme and ultimately to hydroquinone upon electrooxidation is represented in eqs 1 and 2.

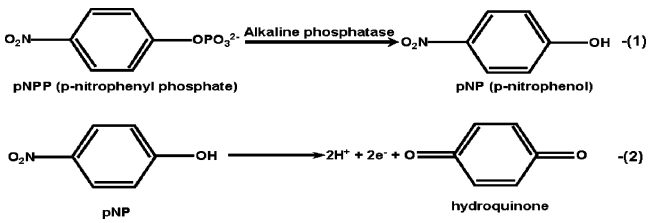

pNP oxidation generally leads to the formation of intermediates, namely benzoquinone and hydroquinone, which are also known to be electroactive. The former is an oxidized compound that can be electroreduced, while the latter is a reduced compound that can be electrooxidized.[23] Figure 5 shows the corresponding voltammograms recorded for the reaction product pNP collected with different concentrations of IL-10 antigen and detector antibody concentration of 5 mM in Tris buffer solution with an incubation time of 1 h. All the measurements were carried out in a smaller test volume of 3 μL at a scan rate of 50 mV/s verses Ag reference electrode. An anodic peak at 0.85 V is observed as a result of the oxidation of the enzymatic product pNP. Careful investigations indicate a dependence of the anodic peak current on the IL-10 concentration. Figure 6a shows the CV recorded with an incubation time of 20 min. No peak for negative control experiments, i.e., the one in which

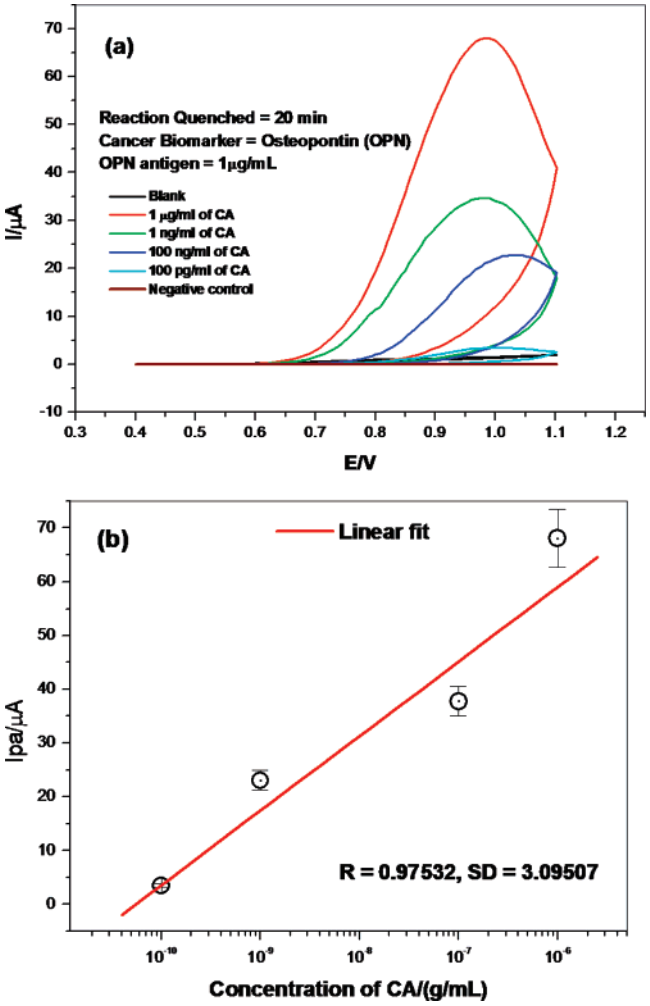

Figure 9. (a) CV recorded for samples with varying concentrations of capture antibody with a fixed concentration of OPN antigen, i.e., 1 μg/mL. (b) The linear dependence of anodic current on the capture antibody concentration.

the complete assay was performed without using the cancer antigens (IL-10), further suggests the selectivity of the present approach. The reaction progress curve for pNPP has been demonstrated to be linear until 40 min.[29] Our results show that with 20 min of reaction time a good separation for the anodic peak current could be obtained and thus was kept constant for all the successive measurements. PBS served as a stopper and was used to control the reaction duration. This addition to the protocol helps in controlling the response and thus looks promising for determining the low concentrations of antigens. The appearance of an anodic peak for IL-10 concentration of 1 ag/mL in the test samples implies the higher sensitivity of the present approach. The difference in the conductivity observed between the blank (plain Tris buffer) and the reaction product is further attributed to the electrolyte composition. A strong dependence of the anodic peak current on the concentration of IL-10 antigen was also observed. Hiller et al. have reported sensitivity of 3.6 pg/mL and 0.6 ng/mL for IL-10 in mice serum with conventional techniques, namely ELISA and Bioassay.[30] Figure 6b shows the corresponding linear dependence of the anodic peak current with the concentration of IL-10 antigen used ($R^2 = 0.98$). However, the slight nonlinearity in the curve could be attributed to the amount and distribution of nanowires over the surface of the silicon substrate. Although the substrates chosen were from the same batch, we anticipate a variation in the nanowires density over the surface, as also revealed in the

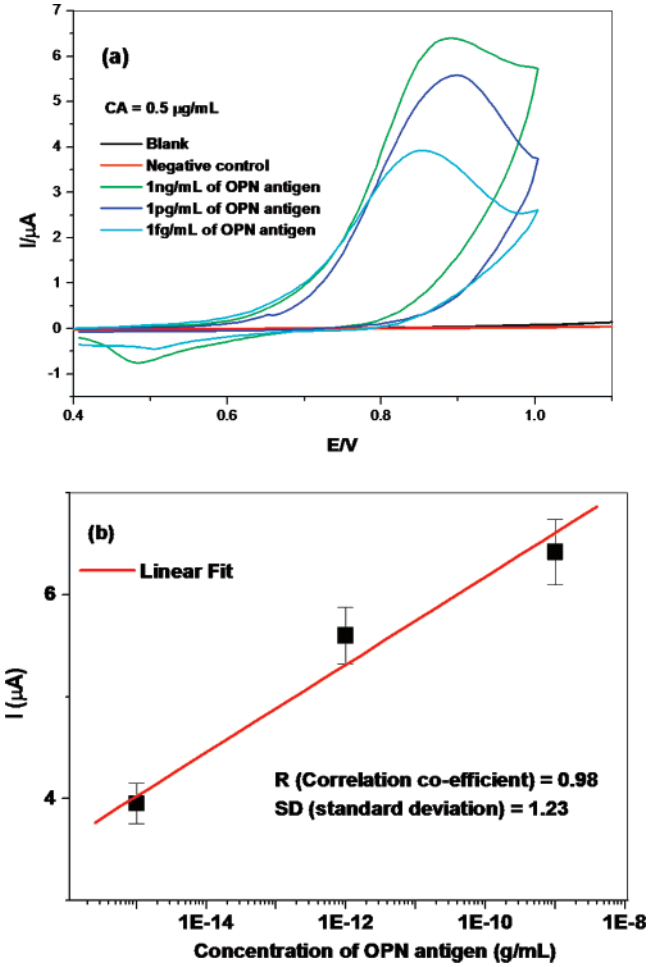

Figure 10. (a) CV plot recorded with varying concentrations of OPN antigen with a fixed CA concentration of 0.5 μg/mL. (b) The linear dependence of anodic current on the antigen concentration.

SEM images of the sample used for 1 ng/mL and 1 pg/mL of IL-10, respectively (Figure 7). The density of wires was calculated to be 9×10^8 and 5×10^8 wires/cm^2 for the sample with 1 ng/mL and 1 pg/mL of IL-10 antigen, respectively. The number density of the wires was estimated by counting the wires in five regions of 1×1 μm^2 of the SEM and averaging them. In addition, careful investigations revealed that the density of nanowires also varied gradually from the periphery toward the center of the substrate. All the experiments were repeated three times with nanowires from a single batch. The variation in the peak current is more evident when the experiments were repeated with nanowires from different batches. This difference could be attributed to the density and distribution of nanowires (aspect ratio), i.e., to the effective AP loading per nanowire.

Biological marker molecules of lung cancer exist in biological fluids in concentrations ranging from pg/mL to sub-ng/mL. The concentration of biomarkers also varies from person to person. The variation of biomarkers from healthy to cancer cells is as little as tens of pg/mL. Generally, progression of cervical cancer is associated with the increased serum level of IL-10. The serum levels of IL-10 are reported to be elevated at stages II and III and dependent directly on the tumor size. For example, Hannigan et al. reported the concentration of IL-10 varying from 109.5 ± 19.6 to 26.4 ± 6 pg/mL from stage I to stage IV of endometrial cancer.[18,19] Hence, there is a need for reliable clinical bioanalytical techniques for accurate measurement of biomarkers in this ultralow concentration range. IL-10 practically is not detectable by standard ELISA in normal serum. Accordingly, real testing was also performed with the clinically relevant samples, i.e., the whole lung serum specimens collected from the individuals who participated in the lung cancer screening study CT clinical trial at the Moffitt Cancer Center. "Normal" serum represents samples from individuals who were not diagnosed with lung cancer at the time of screening with lung imaging modality-helical CT (computer tomography). Additionally, we have used "normal" serum as a dilutant to ensure the presence of assay background proteins/electrolytes, and it was prediluted with PBS at 1:10 ratio.

Figure 8 shows the corresponding electrochemical response recorded for the whole serum with and without IL-10 antigen (1 pg/mL). No appreciable oxidative behavior was observed for the reaction products collected by performing the negative control experiment on the whole serum without antigen. However, the presence of IL-10 antigen even at 1 pg/mL level in the whole serum resulted in an anodic peak at 0.89 V. These results demonstrate the high specificity of the present approach. For 1 pg/mL of IL-10 concentration in serum, the current reaches a maximum at 80 μA, while for the same concentration in test sample, i.e., without serum, the current reaches only 20 μA. The difference in the peak current could be attributed to the presence of biological molecules in the serum samples, making the electrolyte more conducting. Consequently, attenuation in the signal is expected as a result of reduced mass transport. Additionally, the present method also provides the advantage of faster detection; for example, voltammograms were recorded in less than 1 min, including the pipeting of pNP on the electrode and cleaning the electrode surface. It is postulated that the high surface to volume ratio associated with the nanowires and the selective chemical binding chemistry causes the enhancement in the anodic peak current.

For better performance of the sensor, an optimum concentration of both the antigen and corresponding capture antibody must be established. Accordingly, experiments were carried out with varying concentrations of capture antibody and OPN antigen, respectively, in the test samples (buffer solution). Figure 9 shows the CV recorded for samples with varying concentrations of capture antibody with a fixed concentration of OPN antigen, i.e., 1 μg/mL. As the antigen concentration is higher, 100 pg/mL of capture antibody also resulted in the appreciable anodic peak current. Figure 9b shows the linear dependence and Figure 10a shows the CV plot recorded with varying concentrations of antigen with a fixed capture antibody concentration of 0.5 μg/mL. Figure 10b shows a good linear dependence with respect to antigen concentration that can be fitted to a linear equation with slope $=$ 0.41 and intercept at 3.69, respectively. A correlation coefficient and the standard deviation as derived from the linear fit is 0.98 ($R^2 = 0.96$) and 1.23, respectively. Thus, it is evident that both the antigen and antibody concentration have a vital impact on the anodic peak current. pNP can therefore be quantified by measurement of the height of the peak current, thereby giving the concentration of cancer antigens. Moreover, pNP solutions have indefinite stability at room temperature and need not be degassed for storage.

Conclusions

In summary, we demonstrated the use of silica nanowires as an effective template for the enzyme immunoassay. More importantly, simple enzymatic reaction between the AP enzyme and the pNPP was used to detect IL-10 concentration down to 1 fg/mL in ideal and 1 pg/mL in clinically relevant samples of lung serum. Both the capture antibody concentration and the

antigen concentration have a strong influence on the anodic peak current as demonstrated by the results with OPN. Additionally, the electrochemical measurements were carried out in a smaller test volume of 3 μL. Conclusive proof that the change in electrochemical responses observed was due to detection of cancer antigen was obtained through simultaneous use of optical and electrochemical measurements. The density of nanowires also has a significant impact on the response, implying the possibility of further improvement in sensitivity and selectivity upon using nanowires with controlled aspect ratio and density. Our results also demonstrate the feasibility of extending the present approach to other biomarkers by careful choice of nanowire modification techniques. Additionally, the use of aligned nanowires with well-defined aspect ratio and controlled surface modification technique could further help in improving the detection limit. Also, leveraging the electroactive nature of silica nanowires, a multimodal (optical/electrochemical) sensing platform for accurate biodiagnostics could also be easily implemented. This can be further extended to develop an integrated system-on-chip (SOC) in which distinct nanowires and surface receptors can be incorporated as individual device element.

Acknowledgment. We thank Dr. Melvyn Tockman for providing us with initial serum samples from participants in the lung cancer screening CT clinical trial at the Moffitt Cancer Center. This research was supported by the NSF-ECS-SGER grant number 0630110 and NSF IGERT grants DGE 0221681.

References and Notes

(1) Patolsky, F.; Zheng, G.; Lieber, C. M. *Nat. Protocol* **2006**, *4*, 1711.
(2) Rosi, N. L.; Mirkin, C. A. *Chem. Rev.* **2005**, *105* (4), 1547.
(3) Cui, Y.; Wei, Q.; Park, H.; Lieber, C. M. *Science* **2001**, *293*, 1289.
(4) Zhang, R. Q.; Lifshitz, Y.; Lee, S. T. *Adv. Mater.* **2003**, *15*, 635.
(5) Almeida, R. V.; Barrios, A. C.; Panspucci, R. R.; Lipson, M. *Nature* **2004**, *431*, 1081.
(6) Zheng, G.; Patolsky, F.; Cui, Y.; Wang, W. U.; Lieber, C. M. *Nat. Biotechnol.* **2005**, *23*, 1294.
(7) Dugas, V.; Chevalier, Y.; Depret, G.; Nesme, X.; Souteyrand, É. *Sens. Actuators B Chem.* **2004**, *101*, 112.
(8) Corrie, S. R.; Lawrie, G. A.; Trau, M. *Langmuir* **2006**, *22* (6), 2731.
(9) Sirbuly, J. D.; Law, M.; Pauzauskie, P.; Yan, H.; Maslov, A. V.; Knudsen, K.; Saykally, R. J.; Yang, P. *Proc. Natl. Acad. Sci. U.S.A.* **2005**, *102*, 7800.
(10) Ferrari, M. *Nat. Rev.* **2005**, *5*, 161.
(11) Sekhar, P. K.; Sambandan, S. N.; Sood, D. K.; Bhansali, S. *Nanotechnology* **2006**, *17*, 4606.
(12) Sood, D. K.; Sekhar, P. K.; Bhansali, S. *Appl. Phys. Lett.* **2006**, *88*, 143110.
(13) Ramgir, N. S.; Sekhar, P.K.; Zajac, A.; Lee, L.; Zhukov, T. A.; Bhansali, S. *Sens. Lett.* **2007**, in press.
(14) Wang, W. U.; Chen, C.; Lin, K. H.; Fang, Y.; Lieber, C. M. *Proc. Natl. Acad. Sci. U.S.A.* **2005**, *102*, 3208.
(15) Valle, R. P. C.; Chavany, C.; Zhukov, T. A.; Jendoubi, M. *Expert Rev. Mol. Diagn.* **2003**, *3*, 55.
(16) Zhukov, T. A.; Dybiec, M.; Zajac, A.; Qian, W.; Song, D. S.; Tockman, M. S.; Phelan, C.; Ostapenko, S.; Sellers, T. Particles 2006 International Conference, Orlando, FL, 13−16 May, 2006.
(17) Moore, K. W.; de Waal Maleft, R.; Coffman, R. L.; O'Garra, A. *Annu. Rev. Immunol.* **2001**, *19*, 683.
(18) Chopra, V.; Dinh, T. V.; Hannigan, E. V. *J. Cancer Res. Clin. Oncol.* **1997**, *123* (3), 167.
(19) Chopra, V.; Dinh, T. V.; Hannigan, E. V. *Cancer Invest.* **1998**, *16* (3), 152.
(20) Yetman, T. J.; Chambers, A. F. *Clin. Exp. Metastasis* **2003**, *20* (1), 85.
(21) Fanjul-Bolado, P.; Gonzalez-Garcia, M. B.; Costa-Garcia, A. *Anal. Bioanal. Chem.* **2006**, *385*, 1202.
(22) Zajac, A.; Song, D. S.; Qian, W.; Zhukov, T. A. *Colloids Surf. B* **2007**, *58*, 309.
(23) Mulchandani, P.; Hangarter, C. M.; Lei, Y.; Chen, W.; Mulchandani, A. *Biosens. Bioelec.* **2005**, *21*, 523.
(24) Niwa, O.; Yan, X.; Halsall, B.; Heineman, W. R. *Anal. Chem.* **1993**, *65*, 1559.
(25) Bakker, E.; Qin, Y. *Anal. Chem.* **2006**, *78*, 3965.
(26) Abdelali, R.; Magali, B.; Claude, B. *Phy. Rev. B* **2003**, *68*, 184202.
(27) Laughlin, R. B.; Joannopoulos, J. D. *Phy. Rev. B* **1977**, *16*, 2942.
(28) Khan, M. A.; Masudul Hassan, M. J. *Appl. Polym. Sci.* **2006**, *100* (5), 4142.
(29) Thompson, R. Q.; Barone, G. C.; Halsall, H. B.; Heineman, W. R. *Anal. Biochem.* **1991**, *192*, 90.
(30) Hillyer, L. M.; Woodward, B. *Am. J. Physiol. Regul. Integr. Comp. Physiol.* **2003**, *285*, R1514.